Purdue University
Purdue e-Pubs

International High Performance Buildings Conference | School of Mechanical Engineering

July 2018

Domestic Dishwasher Simulated Energy Efficiency Evaluation Using Thermoelectric Heat Pump for Water Heating and Dish Drying

Ahmad Abu-Heiba
Oak Ridge National Laboratory, United States of America, abuheibaag@ornl.gov

Mini Malhotra
Oak Ridge National Laboratory, United States of America, malhotram@ornl.gov

Kyle R Gluesenkamp
Oak Ridge National Laboratory, United States of America, gluesenkampk@ornl.gov

Viral Patel
Oak Ridge National Laboratory, United States of America, patelvk@ornl.gov

Domestic Dishwasher Simulated Energy Efficiency Evaluation Using Thermoelectric Heat Pump for Water Heating and Dish Drying

Ahmad ABU-HEIBA*, Mini MALHOTRA, Kyle R. GLUESENKAMP, Viral K. PATEL

Oak Ridge National Laboratory[1]
Oak Ridge, TN, USA
abuheibaag@ornl.gov, malhotram@ornl.gov, gluesenkampk@ornl.gov, patelvk@ornl.gov

* Corresponding Author

ABSTRACT

A quasi-steady state, heat and mass transfer lumped-capacitance model was developed to predict the energy consumption and drying performance of domestic dishwashers. A numerical finite element solution was applied, assuming that the following components could each be treated as a lumped thermal capacitance: dish load, tub, wash water, and air in tub. The model was used to predict the energy consumption savings of heating water using a thermoelectric heat pump that extracts heat from a thermal storage medium, and the drying performance of circulating tub air through the cold and then hot side of TE modules.

1. INTRODUCTION

In the U.S., the majority of dishwashers draw hot water and use electric resistance heating to further boost the water temperature. These dishwashers consume about 280 TBtu/year of primary energy, or approximately 1.4% of the total annual residential energy use [1]. Currently available dishwashers achieve improved overall efficiency by using high-efficiency components (pumps, motors, water jets), sophisticated soil sensing and control, improved cabinet insulation and innovative dish racks. Despite these improvements in dishwasher design, the energy consumption due to water heating as a percentage of the overall energy consumption remains high [2]. Efficiency is also hampered by ineffective drying which results in moisture discharge and re-condensing on dishes during drying.

Although the vast majority of currently available dishwashers electrically heat air and water, some recent work has focused on improving energy efficiency by using a vapor-compression heat pump [3-5] or open adsorption system [6, 7]. Despite these, research on further development of dishwasher technology is limited.

The proposed technology aims to reduce the water and air heating component of the energy consumption by using an innovative thermoelectric (TE) heat pump system with thermal storage, as illustrated in Figure 1. TEs are a solid-state heat pump technology consisting of two distinct semiconductors sandwiched together in a thin layer. When a DC current is applied, a temperature difference is created between the two sides of the element, and the TE can be used as a heat pump. During the normal cleaning cycle, water being recirculated in the tub is heated by the TE elements instead of an electric heater. This produces a cooling effect on the back side of the TE elements, cooling a liquid or solid thermal mass. Just before the warmed wash water is drained, it is circulated through the thermal mass. This cools the water before draining and provides a warm heat source for the TE during the next phase. By recovering the heat from the dishwasher drain water in this way, significant energy savings can be achieved.

---

[1]This manuscript has been authored by UT-Battelle, LLC under Contract No. DE-AC05-00OR22725 with the U.S. Department of Energy.

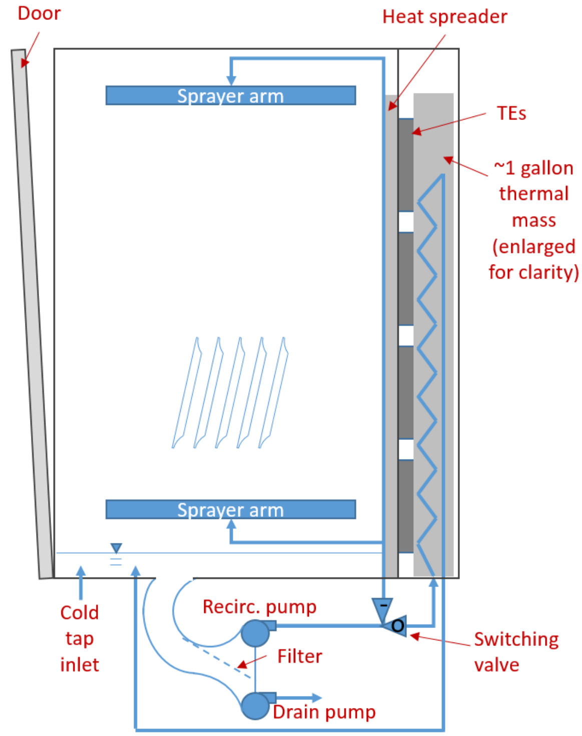

Figure 1. The patented system [8] stores drain water waste heat in a thermal mass, where it can be extracted over time by thermoelectric elements at high efficiency

This paper presents the results of a modeling study on a TE heat recovery dishwasher.

2. MODEL DESCRIPTION

The model uses a quasi-steady state lumped approach to predict the heat and mass transfer. At each time step, first heat and mass transfer between different nodes are calculated based on empirical heat and mass transfer resistances respectively. These fluxes are then used to calculate the temperature and the remaining moisture content of each node at the next time step. The whole cycle is divided into three modes.

The washing and the draining mode are repeated for a number of times to comprise a complete wash cycle. The number of repetitions that was used in this study was arbitrary and will be optimized in future work.

Washing mode

The TE pumps heat from the thermal storage medium and into the water. The water is then sprayed over the load, thus exchanging heat with the walls of the tub and the load. The tub in turn loses heat to the ambient. A network representation of this mode is shown in Figure 2.

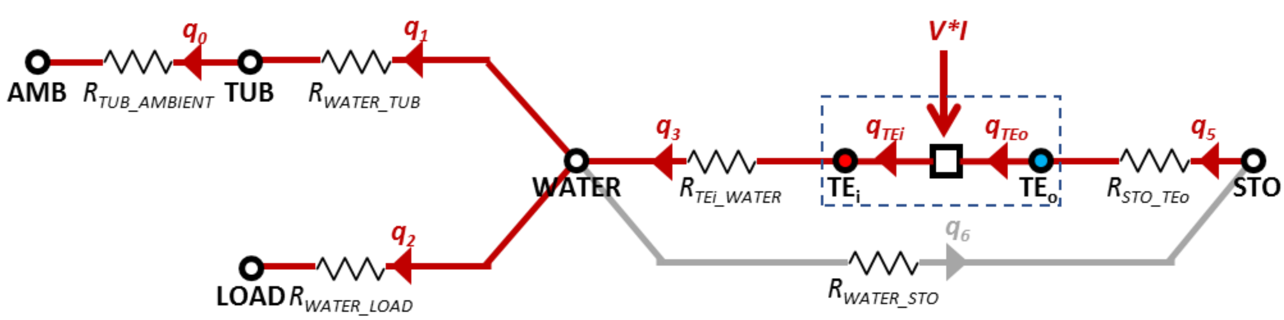

Figure 2. Resistance network diagram of the washing stage. Only red branches are active.

The electric resistance of the TE and its conductance are determined by material properties and geometry of the TE module. They have a fixed value throughout the simulation duration and are given by equations (1-2).

$$R = \frac{L_p \rho_p}{A_p} + \frac{L_n \rho_n}{A_n} \tag{1}$$

$$K = \frac{\lambda_p A_p}{L_p} + \frac{\lambda_n A_n}{L_n} \tag{2}$$

The electric current consumed by the TE is then calculated from the electric resistance and the applied voltage according to equation (3) for each time step *j*. In the general, the voltage is a design variable and can be varied in time according to any control strategy. In this work, the applied voltage is assumed to be constant throughout the simulation duration, so the *j* superscript can be dropped from subsequent equations.

$$I^j = \frac{V^j}{R} \tag{3}$$

The cooling and heating powers are then calculated for each time step *j*, as shown in equations (4-5).

$$q^j_{TEo} = \left[(\alpha_p - \alpha_n) I T^j_{TEo} - K\left(T^j_{TEi} - T^j_{TEo}\right) - \frac{I^2 R}{2} \right] \tag{4}$$

$$q^j_{TEi} = q^j_{TEo} + VI \tag{5}$$

Heat transfer between every node pair is then calculated using the difference in their temperatures and an empirical heat transfer resistance

$$q^j_0 = \frac{T^j_{TUB} - T_{AMBIENT}}{R_{TUB_{AMBIENT}}} \tag{5}$$

$$q^j_1 = \frac{T^j_{WATER} - T^j_{TUB}}{R_{WATER_{TUB}}} \tag{6}$$

$$q^j_2 = \frac{T^j_{WATER} - T^j_{LOAD}}{R_{WATER_{LOAD}}} \tag{7}$$

$$q^j_3 = \frac{T^j_{TEi} - T^j_{WATER}}{R_{TEi_{WATER}}} \tag{8}$$

$$q^j_5 = \frac{{T_{STO}}^j - T^j_{TEo}}{R_{STO\_TEo}} \tag{9}$$

Applying energy conservation to each node then yields its updated temperature

$$q^j_2 = M_{LOAD} * C_{LOAD} * \frac{\left(T^{j+1}_{LOAD} - T^j_{LOAD}\right)}{\Delta t} \tag{10}$$

$$q^j_1 - q^j_0 = M_{TUB} * C_{TUB} * \frac{\left(T^{j+1}_{TUB} - T^j_{TUB}\right)}{\Delta t} \tag{11}$$

$$q_3^j - q_2^j - q_1^j - q_6^j = M_{WATER} * C_{WATER} * \frac{(T_{WATER}^{j+1} - T_{WATER}^j)}{\Delta t} \tag{12}$$

$$q_{TEi}^j - q_3^j = M_{TEi} * C_{TEi} * \frac{(T_{TEi}^{j+1} - T_{TEi}^j)}{\Delta t} \tag{13}$$

$$q_5^j - q_{TEo}^j = M_{TEo} * C_{TEo} * \frac{(T_{TEo}^{j+1} - T_{TEo}^j)}{\Delta t} \tag{14}$$

$$q_6^j - q_5^j = M_{STO} * C_{STO} * \frac{(T_{STO}^{j+1} - T_{STO}^j)}{\Delta t} \tag{15}$$

These calculations are repeated for a specified duration. The duration of the mode is a design variable.

Draining mode

This mode follows each washing mode. Together an occurrence of the washing mode and draining mode can be repeated to complete a wash cycle.

In the drain mode, the water is circulated through the thermal storage medium to recover as much of its heat content as possible before it is drained.

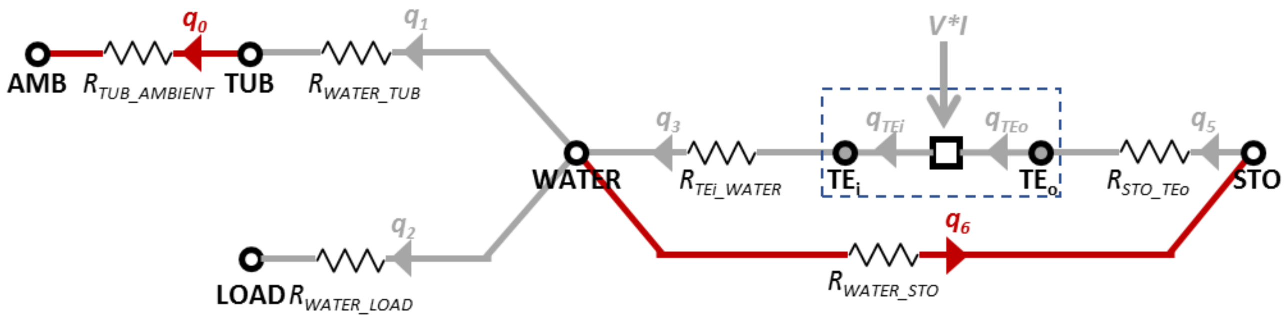

Figure 3. Resistance network diagram of the draining stage. Only red branches are active.

Heat transfer from the water to the storage medium and from the tub walls to the ambient are

$$q_6^j = \frac{T_{WATER}^j - T_{STO}^j}{R_{WATER\_STO}} \tag{16}$$

$$q_0^j = \frac{T_{TUB}^j - T_{AMBIENT}}{R_{TUB_{AMBIENT}}} \tag{17}$$

These heat fluxes are then used to update the temperature of the tub walls, of the thermal storage medium and of the water

Table 1

$$q_6^j = M_{STO} * C_{STO} * \frac{(T_{STO}^{j+1} - T_{STO}^j)}{\Delta t} \tag{18}$$

$$-q_6^j = M_{WATER} * C_{WATER} * \frac{(T_{WATER}^{j+1} - T_{WATER}^j)}{\Delta t} \tag{19}$$

$$q_1^j - q_0^j = M_{TUB} * C_{TUB} * \frac{(T_{TUB}^{j+1} - T_{TUB}^j)}{\Delta t} \tag{20}$$

These calculations are repeated for a specified length of time that is an input to the model. The durations used in the current study are arbitrary. In future work they will be optimized and validated experimentally.

Drying stage

This stage follows the last draining mode (the end of the wash cycle). Heat is pumped from the air contained in the tub and into the thermal storage medium. The tub walls also lose heat to the ambient. As the TE operates, its inner (tub-side) temperature decreases. As the process continues, the temperature of the inner side of the TE drops below the dew point of the air in the tub. Water vapor in the air then condenses on the TE, reducing the humidity of the air. This in turn causes water vapor to transfer into the air from the tub walls and the load. In this stage, ambient air is assumed to be blown into the tub, replacing some of the air in the tub. A resistance network of this stage is shown in Figure 4.

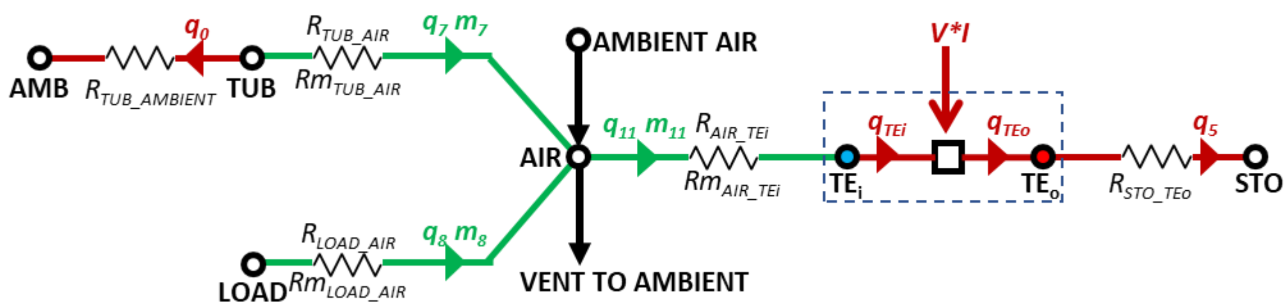

Figure 4. Resistance network diagram of the drying cycle. Green branches represent combined mass and heat transfer while red branches represent only het transfer.

First, the heat pumped by the TE is calculated in the same manner that was detailed in the wash stage. Then, the temperature and the humidity of the air in the tub is updated to reflect the effect of mixing with the ambient air

$$M_{AIR} * T^j_{AIR_{UPDATED}} = (M_{AIR} - \dot{m}_{AMBIENT} * \Delta t) * T^j_{AIR_{OLD}} + \dot{m}_{AMBIENT} * \Delta t * T_{AMBIENT} \tag{21}$$

$$M_{AIR} * W^j_{AIR_{UPDATED}} = (M_{AIR} - \dot{m}_{AMBIENT} * \Delta t) * W^j_{AIR_{OLD}} + \dot{m}_{AMBIENT} * \Delta t * W_{AMBIENT} \tag{22}$$

These updated values are used in the rest of the calculations. For simplicity, the subscript "UPDATED" will be dropped from here on. The amount of water vapor in the air is calculated

$$M^j_{VAP\_IN\_AIR} = W^j_{AIR} * M_{AIR} \tag{23}$$

Mass transfer is calculated using the difference in vapor pressure and empirical mass transfer resistances. The vapor pressure of water on the load, on the inner side of the TE and on the wall of the tub are calculated. They are taken as the saturation pressure of water at the temperature of their corresponding node. The saturation pressure is calculated using ASHRAE equation for saturation pressure over liquid water

$$\ln(p_{ws}) = \frac{C_8}{T} + C_9 + C_{10}T + C_{11}T^2 + C_{12}T^3 + C_{13}\ln(T) \tag{24}$$

Where

$C_8 = -5.800\,220\,6\text{ E}+03$ $\quad C_9 = 1.391\,499\,3\text{ E}+00$

$C_{10} = -4.864\,023\,9\text{ E}-02$ $\quad C_{11} = 4.176\,476\,8\text{ E}-05$

$C_{12} = -1.445\,209\,3\text{ E}{-08}$ $C_{13} = 6.545\,967\,3\text{ E}{+00}$

Vapor pressure of the water in the air was calculated by multiplying the saturation pressure over water at the temperature of the air by the relative humidity of the air. Mass transfers between different nodes are then calculated and used to update the remaining moisture in each node.

$$m_7^j = \frac{P_{TUB}^j - P_{VAP}^j}{Rm_{TUB\_AIR}} \tag{24}$$

$$-m_7^j = \frac{\left(M_{w_{TUB}}^{j+1} - M_{w_{TUB}}^j\right)}{\Delta t} \tag{25}$$

$$m_8^j = \frac{P_{LOAD}^j - P_{VAP}^j}{Rm_{LOAD_{AIR}}} \tag{26}$$

$$-m_8^j = \frac{\left(M_{w_{LOAD}}^{j+1} - M_{w_{LOAD}}^j\right)}{\Delta t} \tag{27}$$

$$m_{11}^j = \frac{P_{VAP}^j - P_{TEi}^j}{Rm_{TEi_{AIR}}} \tag{28}$$

$$m_7^j + m_8^j - m_{11}^j = \frac{\left(M_{VAP_{IN_{AIR}}}^{j+1} - M_{VAP_{IN_{AIR}}}^j\right)}{\Delta t} \tag{29}$$

Heat transfer between each pair of nodes is then calculated based on the difference of their temperatures and empirical heat transfer resistance. Conservation of energy was then applied on each node to update its temperature for the next time step.

$$q_5^j = \frac{{T_{TEo}}^j - T_{STO}^j}{R_{STO\_TEo}} \tag{30}$$

$$q_{TEo}^j - q_5^j = M_{TEo} * C_{TEo} * \frac{\left(T_{TEo}^{j+1} - T_{TEo}^j\right)}{\Delta t} \tag{31}$$

$$q_5^j = M_{STO} * C_{STO} * \frac{\left(T_{STO}^{j+1} - T_{STO}^j\right)}{\Delta t} \tag{32}$$

$$q_{11}^j = \frac{T_{AIR}^j - T_{TEi}^j}{R_{TEi\_AIR}} \tag{33}$$

$$q_{11}^j - q_{TEi}^j + m_{11}^j * h_{fg} = M_{TE\mathrm{i}} * C_{TEi} * \frac{\left(T_{TEi}^{j+1} - T_{TEi}^j\right)}{\Delta t} \tag{34}$$

$$q_7^j = \frac{T_{TUB}^j - T_{AIR}^j}{R_{TUB\_AIR}} \tag{35}$$

$$q_0^j = \frac{T_{TUB}^j - T_{AMBIENT}}{R_{TUB_{AMBIENT}}} \tag{36}$$

$$-q_7 - q_0 - m_{11}^j * h_{fg} = M_{TUB} * C_{TUB} * \frac{(T_{TUB}^{j+1} - T_{TUB}^j)}{\Delta t} \quad (37)$$

$$q_8^j = \frac{T_{LOAD}^j - T_{AIR}^j}{R_{LOAD_{AIR}}} \quad (38)$$

$$-q_8^j - m_{11}^j * h_{fg} = M_{LOAD} * C_{LOAD} * \frac{(T_{LOAD}^{j+1} - T_{LOAD}^j)}{\Delta t} \quad (39)$$

$$C_{AIR} = 1000 + 1820 * W_{AIR} \quad (40)$$

$$q_7^j + q_8^j - q_{11}^j + m_{11}^j * h_{fg} = M_{AIR} * C_{AIR} * \frac{(T_{AIR}^{j+1} - T_{AIR}^j)}{\Delta t} \quad (41)$$

These calculation steps were repeated until all water on the load was evaporated into the tub air.

3. RESULTS AND DISCUSSION

The mass and heat transfer resistance values that were used to run the model were best guess values. The wash cycle was comprised of 4 repetitions of wash and drain modes. The model for range of voltage from 10 to 100 in 10 volts increment. The following graphs will show some of the key performance trends.

Figure 5, Figure 6 and Figure 7 show key temperature trends during the wash cycle. The higher the voltage is, the higher the swing in the temperature.

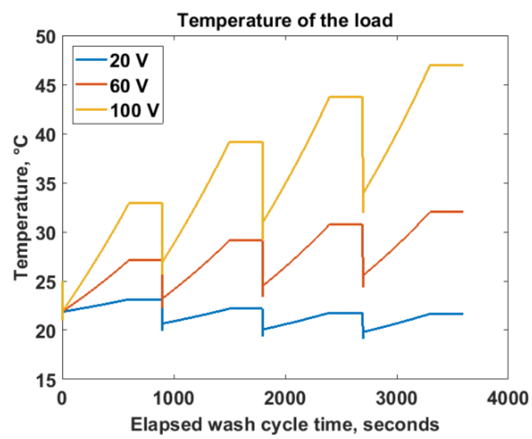

Figure 5. Temperature trend of the load at different supply voltages during wash cycle.

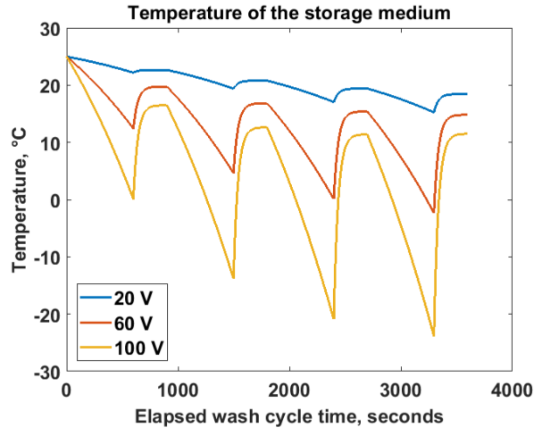

Figure 6. Temperature trend of the thermal storage medium at different voltages during wash cycle.

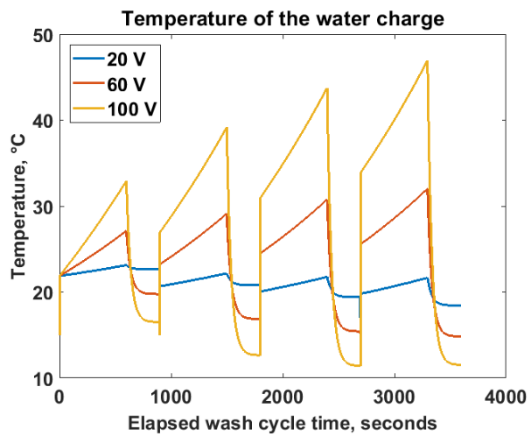

Figure 7. Temperature trend of the water charge at different voltages during wash cycle.

Figure 8 and Figure 9 show the temperature trends of the load and the thermal storage medium during the drying mode for different voltages.

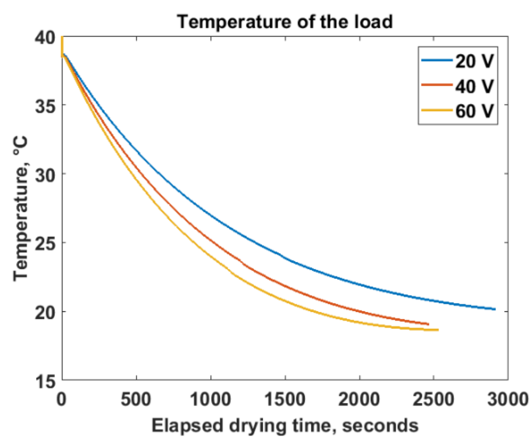

Figure 8. Temperature trend of the load at different voltages during drying mode.

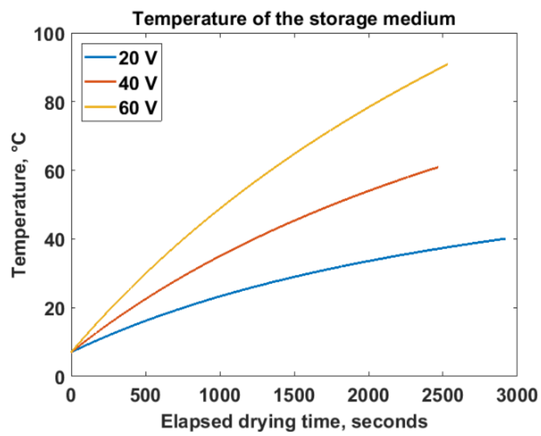

Figure 9. Temperature trend of the thermal storage medium at different voltages during drying mode.

The higher the voltage is, the shorter the drying time is thought to be. Interestingly, Figure 10 shows a different trend. Increasing the voltage reduces the drying time until a certain point where increasing voltage does not reduce the drying time anymore. Past that point, increasing the voltage in fact increases the drying time before the trend reverses course again. This may be due to extremely hot temperatures developed in the thermal storage. Meanwhile, energy consumption during drying mode increases monotonically with increasing voltage.

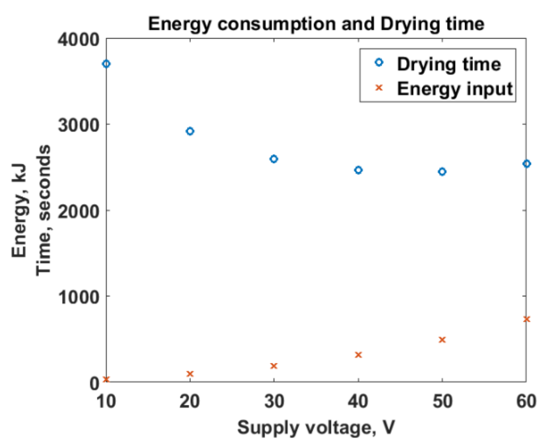

Figure 10. Effect of voltage on energy consumption during drying mode and drying time.

4. CONCLUSION

A lumped capacitance, quasi-steady state numerical model of a novel thermoelectric dishwasher with integrated thermal storage was developed. The model predicts energy consumption for the washing cycle and the drying mode, and the duration of the drying mode. Model results were obtained under a simple set of assumptions about the wash cycle: 4 equal duration wash events, each with 1 gallon of water. Thermoelectric heat pump applied voltage was varied parametrically. The highest voltage evaluated heated the wash water to only 47 C, while the thermal storage was cooled below freezing. Therefore, a larger thermal storage and/or some electric resistance heating may be required for favorable operation. In the future work, the design parameters in the model will be more explored further.

NOMENCLATURE

C	specific heat capacity, $kJ^1kg^{-1}K^{-1}$
K	thermal conductivity of TE module, $W^1m^{-1}K^{-1}$
h_{fg}	latent heat of vaporization of water
I	current
L_n	length of n-type nodes, m
L_p	length of p-type nodes, m
m	mass flow rate, kg/s
M	mass, kg
q	heat flow, kW
R	heat transfer resistance, K^1W^{-1}; resistance of TE module, OhmRm mass transfer resistance, $Pa^1kg^{-1}s^1$
t	time, s
T	temperature, °C
TE	thermoelectric module
V	voltage
Δt	timestep used in model
ρ	electrical resistivity of TE material

Subscript

AIR	air inside tube
LOAD	dishware
STO	thermal storage mass
TEi	inside of TEs (inside tub)
TEo	outside of TEs
TUB	walls of dishwasher

Superscript

j	timestep

ACKNOWLEDGEMENTS

This work was sponsored by the U. S. Department of Energy's Building Technologies Office under Contract No. DE-AC05-00OR22725 with UT-Battelle, LLC. The authors would also like to acknowledge Mr. Antonio Bouza, Technology Manager – HVAC&R, Water Heating, and Appliance, U.S. Department of Energy Building Technologies Office.

The authors would also like to acknowledge Guolian Wu of Samsung Electronics America for his valuable input on the research.

REFERENCES

[1] EIA, 2018, "Baseline Energy Calculator," https://trynthink.github.io/scout/calculator.html, U.S. Energy Information Administration.

[2] Hoak, D. E., Parker, D. S., and Hermelink, A. H., 2008, "How energy efficient are modern dishwashers?," Proc. ACEEE Summer Study on Energy Efficiency in Buildings, Pacific Grove, CA, ACEEE.

[3] Bengtsson, P., Berghel, J., and Renström, R., 2015, "A household dishwasher heated by a heat pump system using an energy storage unit with water as the heat source," International Journal of Refrigeration, 49, pp. 19-27.

[4] Bengtsson, P., and Berghel, J., 2016, "Study of using a capillary tube in a heat pump dishwasher with transient heating," International Journal of Refrigeration, 67, pp. 1-9.

[5] Bengtsson, P., and Eikevik, T., 2016, "Reducing the global warming impact of a household heat pump dishwasher using hydrocarbon refrigerants," Applied Thermal Engineering, 99, pp. 1295-1302.

[6] Hauer, A., and Fischer, F., 2011, "Open Adsorption System for an Energy Efficient Dishwasher," Chemie Ingenieur Technik, 83(1-2), pp. 61-66.

[7] Santori, G., Frazzica, A., Freni, A., Galieni, M., Bonaccorsi, L., Polonara, F., and Restuccia, G., 2013, "Optimization and testing on an adsorption dishwasher," Energy, 50, pp. 170-176.

[8] Gluesenkamp, K. R., 2018, Configuration of Dishwasher to Improve Energy Efficiency of Water Heating, USPTO, Publication number Application number US Patent 9,949,611, granted April 24, 2018.